Published OnlineFirst January 26, 2012; DOI: 10.1158/0008-5472.CAN-11-2905

Microenvironment and Immunology

Cancer Research

Myeloid Progenitor Cells in the Premetastatic Lung Promote Metastases by Inducing Mesenchymal to Epithelial Transition

Dingcheng Gao[1,2], Natasha Joshi[1,2], Hyejin Choi[1,2], Seongho Ryu[1,2], Mary Hahn[1,2], Raul Catena[1,2], Helen Sadik[6], Pedram Argani[6], Patrick Wagner[3], Linda T. Vahdat[4], Jeffrey L. Port[1], Brendon Stiles[1], Saraswati Sukumar[6], Nasser K. Altorki[1], Shahin Rafii[5], and Vivek Mittal[1,2]

Abstract

Tumors systemically initiate metastatic niches in distant target metastatic organs. These niches, composed of bone marrow–derived hematopoietic cells, provide permissive conditions for future metastases. However, the mechanisms by which these cells mediate outgrowth of metastatic tumor cells are not completely known. Using mouse models of spontaneous breast cancer, we show enhanced recruitment of bone marrow–derived $CD11b^{+}Gr1^{+}$ myeloid progenitor cells in the premetastatic lungs. Gene expression profiling revealed that the myeloid cells from metastatic lungs express versican, an extracellular matrix proteoglycan. Notably, versican in metastatic lungs was mainly contributed by the $CD11b^{+}Ly6C^{high}$ monocytic fraction of the myeloid cells and not the tumor cells or other stromal cells. Versican knockdown in the bone marrow significantly impaired lung metastases *in vivo*, without impacting their recruitment to the lungs or altering the immune microenvironment. Versican stimulated mesenchymal to epithelial transition of metastatic tumor cells by attenuating phospho-Smad2 levels, which resulted in elevated cell proliferation and accelerated metastases. Analysis of clinical specimens showed elevated versican expression within the metastatic lung of patients with breast cancer. Together, our findings suggest that selectively targeting tumor-elicited myeloid cells or versican represents a potential therapeutic strategy for combating metastatic disease. *Cancer Res; 72(6); 1384–94. ©2012 AACR.*

Introduction

Malignant tumors colonize distal target organs to establish metastases (1, 2) causing more than 90% of human cancer-related deaths (3). Many studies have investigated the cancer cell intrinsic molecular mechanisms and the extrinsic microenvironmental factors that enhance the metastatic potential of primary tumor cells (3, 4). Notably, activation of epithelial to mesenchymal transition (EMT), a developmental program, endows metastatic properties upon cancer cells to promote invasion, migration, and subsequent dissemination (5).

Following dissemination, the establishment of metastatic lesions depends on the organ-colonizing properties of disseminated tumor cells as well as on permissive conditions or the "metastatic niche" that may be present in the microenvironment of target organs (3, 6). Notably, bone marrow–derived cells are recruited to the metastatic organs to support initiation of metastases (7), and angiogenesis-mediated progression of micrometastases to macrometastases (8). Although some of these stromal contributors have been identified, effective therapies still require a more comprehensive understanding of the complex molecular and cellular network of tumor–stroma interactions in the metastatic organ that contribute to the formation of macrometastases. Transitions between epithelial and mesenchymal states have crucial roles in both embryonic development and cancer. An apparent contradiction of the association between EMT and metastasis comes from repeated observations that distant metastases derived from primary carcinomas are largely composed of cancer cells showing an epithelial phenotype closely resembling that of the cancer cells in the primary tumor. This has led to speculation that the disseminated mesenchymal tumor cells recruited to the target organs may undergo mesenchymal to epithelial transition (MET) which would favor metastases formation (9). However, the MET cascade has not been recapitulated in animal models, and the cellular and molecular regulators that promote MET remain unknown. In this study, we have focused on events in the distal metastatic organ and sought to identify the microenvironmental factors that affect metastatic outgrowth.

Materials and Methods

Mice

FVB/n, FVB.Cg-Tg (ACTB-EGFP) B5Nagy/J, and MMTV-PyVT mice were obtained from The Jackson Laboratory. Male

Authors' Affiliations: [1]Department of Cardiothoracic Surgery and Neuberger Berman Lung Cancer Center, Departments of [2]Cell and Developmental Biology, [3]Pathology, and [4]Medicine, [5]HHMI, Department of Genetic Medicine, Weill Cornell Medical College of Cornell University, New York, New York; and [6]Sidney Kimmel Comprehensive Cancer Center at Johns Hopkins, Baltimore, Maryland

Note: Supplementary data for this article are available at Cancer Research Online (http://cancerres.aacrjournals.org/).

Corresponding Authors: Vivek Mittal, Weill Cornell Medical College of Cornell University, 1300 York Avenue, Room 603C, New York, NY 10065. Phone: 212-746-9401; Fax: 212-746-9393; E-mail: vim2010@med.cornell.edu; and Dingcheng Gao, Phone: 212-746-9450; E-mail: dig2009@med.cornell.edu

doi: 10.1158/0008-5472.CAN-11-2905

Published OnlineFirst January 26, 2012; DOI: 10.1158/0008-5472.CAN-11-2905

MMTV-PyMT transgenic mice were bred with wild-type FVB/N females. Female offsprings (3 weeks) were genotyped to identify mice carrying the PyMT transgene. The positive mice spontaneously develop mammary tumors by 6 to 7 weeks of age and pulmonary metastases by 10 to 12 weeks of age. To quantify lung metastases in MMTV-PyMT mice, serial lung sections (at least 10) were prepared and stained with hematoxylin and eosin. Within the stained sections, areas depicting metastatic lesions and total lung were measured with ImageJ software.

Cell lines

The human breast cancer cell line (MDA-MB-231) was obtained from American Type Culture Collection (ATCC), a kind gift from Dr. Randy Watnick (Harvard Medical School, Boston, MA). Cultures were resuscitated from stocks frozen at low passage within 6 months of purchase. Cell authentication was conducted at ATCC by short tandem repeat profiling, cell morphology monitoring, karyotyping, and the ATCC cytochrome *c* oxidase I (COI) assays. The morphology and metastatic behavior of MDA-MB-231 cells were tested in our laboratory and the laboratory of Dr. Watnick. Cells were cultured in Dulbecco's Modified Eagle's Media with 10% FBS, 5 mmol/L glutamine, and 1% penicillin/streptomycin. Versican-expressing cells (MDA-Vcn) were generated by transfection with a construct carrying the secreted form of human versican cDNA (pSecTag-V1, a gift from Dr. Zimmermann, University of Zurich, Zurich, Switzerland; ref. 10). Stably transfected cells were obtained by selecting cells with Zeocin (200 μg/mL). MDA-Cont cells were obtained by transfection of MDA-MB-231 cells with control empty vector and selected through the same procedure. MDA-MB-231 cells were also labeled with luciferase-RFP (red fluorescent protein) fusion protein for bioluminescent imaging *in vivo*.

Human samples

Human normal lung tissues ($n = 5$) were obtained from ILSbio LLC. Human lungs bearing metastases from patients with breast cancer were obtained from Department of Cardiothoracic Surgery, Weill Cornell Medical College (New York), consented according to approved Institutional Review Board (IRB) protocols from the institution. Metastatic tissues from the lungs of patients with breast cancer ($n = 11$) were obtained in the form of a tissue microarray from the group of P. Argani and S. Sukumar at Johns Hopkins University School of Medicine, Baltimore, MD.

Short hairpin RNA design and lentiviral vector generation

Mir30-based short hairpin RNAs (shRNA) targeting mouse versican (V0/V1 isoform) were designed and cloned into the *Xho*I/*Eco*RI site of the lentiviral construct pGIPZ (OpenBiosystem). Multiple hairpin constructs were screened for effective knockdown of versican. The 22-mer targeting sequence that resulted in efficient knockdown included 5′-ACACCAGAATTAGAAAGTTCAA-3′ (shVcn1) and 5′-AGCACCTTGTCTGATGGCCAAG-3′ (shVcn2), shRNA targeting firefly luciferase served as a nonspecific control. Lentivirus was generated and concentrated using standard protocols. Lentiviral transductions of Lin^- bone marrow cells were conducted as described (8).

Bone marrow transplantation of mice

Bone marrow cells were harvested by flushing femurs and tibias of donor animals. Bone marrow transplantation was conducted by injecting 1×10^7 total bone marrow cells via tail vein into lethally irradiated (900 radians) recipients as described (8).

Immunostaining and microscopy

Fixed tissue sections (30 μm) were stained with fluorescence-labeled antibodies against CD11b (clone ICRF44), CD33 (Cat#555459, BD), Gr1 (Clone RB6-8C5), versican (Cat#V5639, Sigma and Clone 2B1 Seikagaku), and PyMT (NB 100-2749, Novus) according to standard protocols. Fluorescent images were obtained using an Axiovert 200M fluorescent microscope (Carl Zeiss Inc.). For versican staining, sections were first treated with chondroitinase ABC (Sigma) overnight and then incubated with an anti-versican antibody (Cat#V5639, Sigma). For immunohistochemistry, the antibody labeling was visualized using the DAKO Envision system (DAKO). Images were taken with an Olympus BX51 microscope coupled with QCapture software (Olympus).

Conditioned medium, purified versican, and cell proliferation assay

Flow cytometry–sorted $CD11b^+Gr1^+$ cells from MMTV-PyMT mice (10 weeks old) were cultured in RPMI with 10% FBS with a density of 100,000 cells/mL in 6-well plates. Conditioned medium was harvested after 2 days. For versican purification, 293T cells were transfected with construct carrying 6× His-tagged human versican (V1 isoform). Supernatant was harvested 5 days after transfection. Versican was purified with Ni-NTA Fast Start Kit (Qiagen Inc). For cell proliferation assay, cells were treated with the conditioned medium, purified versican (2.5 μg/mL), or normal growth medium for 3 days. EdUrd (5-ethynyl-2′-deoxyuridine; 10 nmol/L) was administered to culture medium for 30 minutes. The incorporation of EdUrd was detected using the Click-iT EdUrd Cell Proliferation Assay Kit (Invitrogen Inc.) and analyzed by flow cytometry.

Statistical analysis

Results are expressed as mean ± SD. Analyses of different treatment groups were conducted using the Student T test using the GraphPad Prism statistical program. P values <0.05 were considered significant. Error bars depict SD, except indicated otherwise.

Supplementary methods

Supplementary methods include flow cytometric analysis, real time PCR analysis including primer sequences (Supplementary Table S1), and Western blot analysis.

Published OnlineFirst January 26, 2012; DOI: 10.1158/0008-5472.CAN-11-2905

Results

Bone marrow–derived CD11b$^+$Gr1$^+$ myeloid cells are recruited in the metastatic lungs

To determine the contribution of the bone marrow–derived cells to the metastatic lung, we transplanted MMTV-PyMT transgenic mice (11) with syngeneic GFP$^+$ bone marrow as previously described (8, 12). In these animals, spontaneous breast tumors (6–7 weeks of age) metastasize to the lungs and form micrometastases (11–12 weeks of age) and macrometastases by week 16 (8, 12). Flow cytometric analysis showed increased recruitment (~3-fold) of GFP$^+$ bone marrow–derived cells in the MMTV-PyMT metastatic lungs compared with wild-type (36.3% ± 4.3% and 12.4% ± 4.2% of total lung cells, respectively; Fig. 1A). Notably, in the metastatic lung, the recruited GFP$^+$ bone marrow–derived cells were predominantly CD11b$^+$Gr1$^+$ myeloid progenitor cells (>50%; Fig. 1A) as determined by flow cytometry and immunostaining (Fig. 1B).

We next conducted a kinetic analysis to determine the recruitment of these cells as a function of metastases progression. Notably, the recruitment of CD11b$^+$Gr1$^+$ cells was observed in the premetastatic lung of 8-week-old MMTV-PyMT mice before the appearance of metastases, and increasing numbers of CD11b$^+$Gr1$^+$ cells were associated with the progression of metastases (Fig. 1C and Supplementary Fig. S1). Conspicuously, compared with the metastatic lung, the numbers of CD11b$^+$Gr1$^+$ myeloid cells were less abundant in the primary tumor. The CD11b$^+$ cells in primary tumor tissue were predominantly Gr1$^-$F4/80$^+$ macrophages (approximately 80%) in contrast to the Gr1$^+$F4/80$^-$ myeloid cells in metastatic lung (Fig. 1D). Such enhanced recruitment of myeloid cells specifically in the metastatic lungs suggests that they may be involved in promoting outgrowth of tumor cells.

Versican is expressed by myeloid cells in the metastatic lung

To determine the molecular mechanisms by which the CD11b$^+$Gr1$^+$ myeloid cells may contribute to lung metastasis, we conducted gene expression profiling of flow cytometry–sorted CD11b$^+$Gr1$^+$ cells from metastatic and wild-type lungs. A cluster of differentially upregulated genes was identified in the myeloid cells from metastatic lungs (Fig. 2A). Of the candidate genes, we focused on versican, an extracellular matrix chondroitin sulfate proteoglycan (13), expressed by tumor stromal cells (14–19). However, the biologic function of versican *in vivo* particularly in the metastatic organs has not been elucidated. RT-PCR analysis showed an approximately 5-fold increase in versican expression in the metastatic lung (ML, total) compared with controls (WT, total; Fig. 2B). In the metastatic lungs, versican expression was confined to CD11b$^+$Gr1$^+$ cells and not to the CD11b$^-$Gr1$^-$ stromal cells

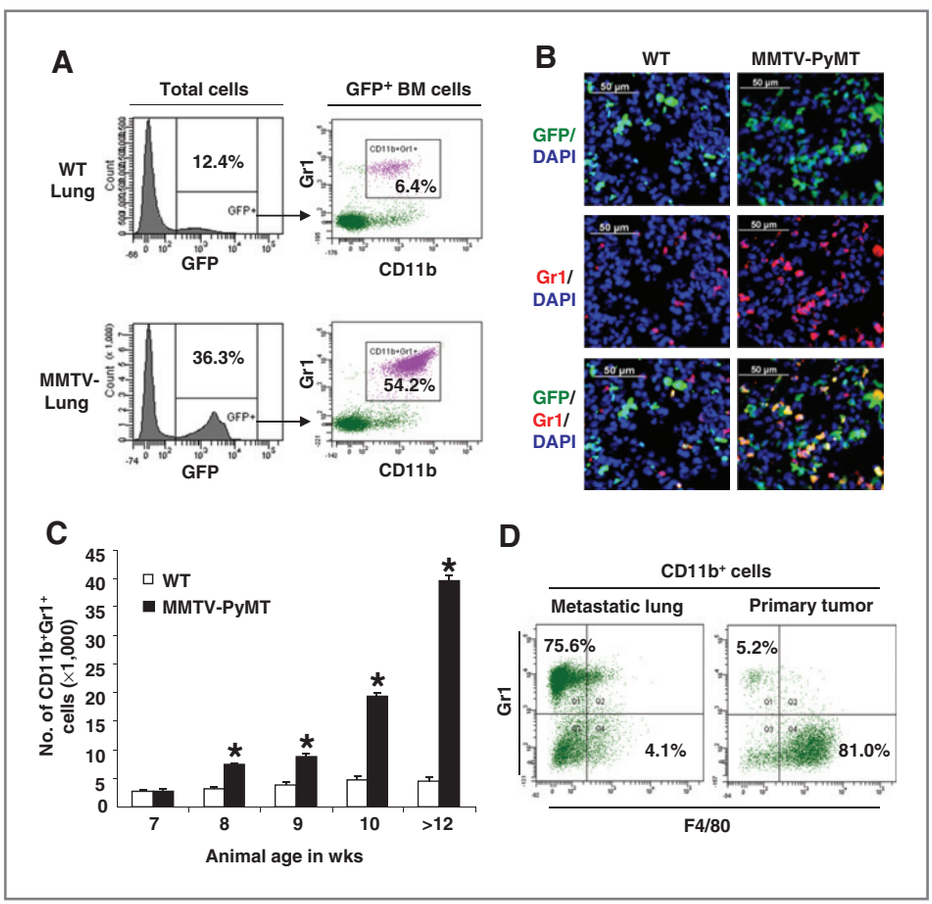

Figure 1. Myeloid cells are recruited to the lung in MMTV-PyMT mice. A, flow cytometric plots showing increased recruitment of bone marrow–derived (GFP$^+$) CD11b$^+$Gr1$^+$ myeloid cells in the lungs of MMTV-PyMT mice (12 weeks old) compared with wild-type (WT) mice. Representative plots were derived from 3 independent experiments. BM, bone marrow. B, immunostaining showing increased recruitment of bone marrow–derived GFP$^+$Gr1$^+$ cells in the lungs of MMTV-PyMT mice compared with WT mice. DAPI, 4′,6-diamidino-2-phenylindole. C, kinetic analysis of the recruitment of CD11b$^+$Gr1$^+$ myeloid cells in the lungs of MMTV-PyMT mice (age in weeks). The numbers of CD11b$^+$Gr1$^+$ cells were normalized to 1 × 10^5 total lung cells analyzed per animal. Mean ± SD. *, $P < 0.01$ as compared with WT mice of same age. D, flow cytometric analysis showing the majority of myeloid cells are Gr1$^+$F4/80$^-$ in the metastatic lung but are Gr1$^-$F4/80$^+$ macrophages in the primary tumors.

Published OnlineFirst January 26, 2012; DOI: 10.1158/0008-5472.CAN-11-2905

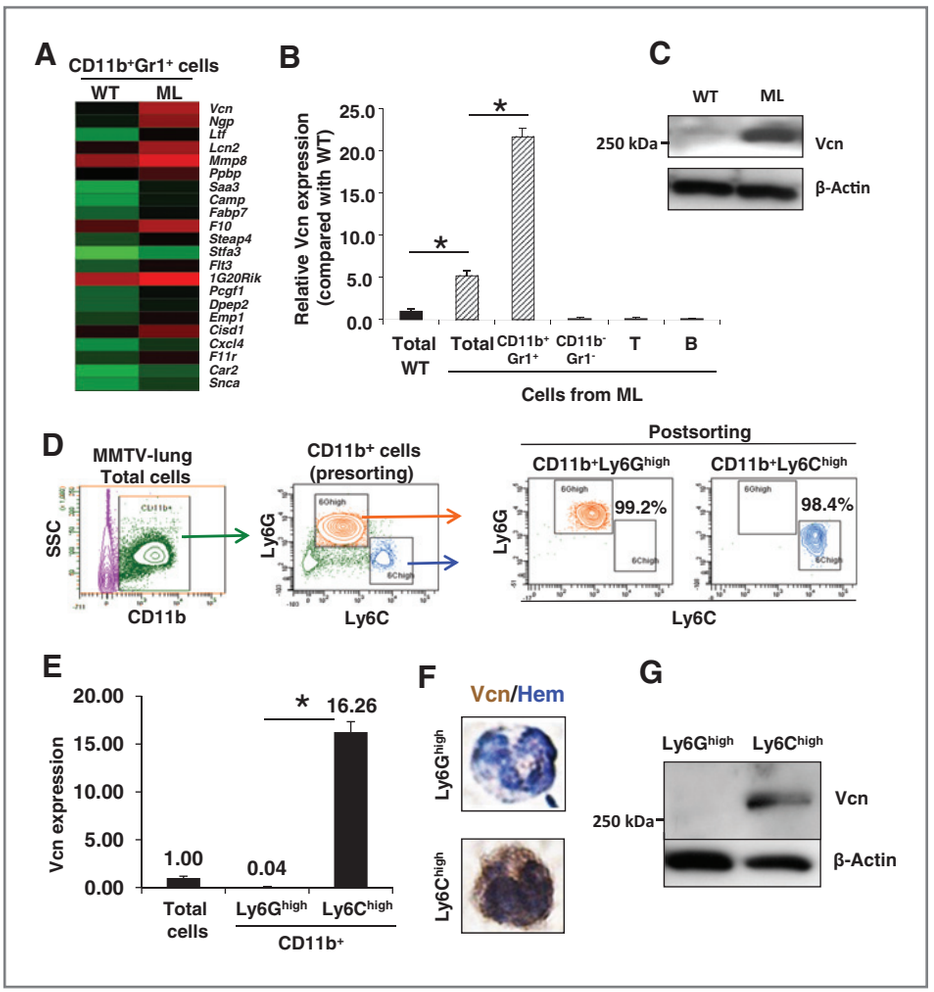

Figure 2. Versican is expressed by CD11b$^+$Ly6C^{high} myeloid cells in the metastatic lung. A, heatmap obtained from gene expression profiling of CD11b$^+$Gr1$^+$ cells sorted from wild-type (WT) lungs and metastatic lungs (ML). Each row represents a differentially upregulated gene ($\geq$ 2-fold) in ML samples, and each column represents data from one comparison (average of 3 biologic replicates). Red, high expression; green, low expression. B, RT-PCR showing versican (Vcn) expression in Gr1$^+$ myeloid cells, Gr1$^-$ stromal cells, T cells (CD3$^+$), and B cells (B220$^+$) sorted from WT or ML (representative data from 2 individual experiments). Versican expression was normalized to the internal control (GAPDH; glyceraldehyde-3-phosphate dehydrogenase). The relative expression level is shown as compared with WT lung. *, $P < 0.01$ as indicated. C, Western blot analysis showing versican levels in the lungs from MMTV-PyMT mice and control mice. D, left, flow cytometric sorting of CD11b$^+$Ly6G^{high} and CD11b$^+$Ly6C^{high} cells from the lungs of MMTV-PyMT mice. Right, flow cytometry showing purity of the postsorted cells. SSC, side scatter. E, RT-PCR of versican expression in CD11b$^+$Ly6G^{high} and CD11b$^+$Ly6C^{high} cells and total cells from metastatic lungs. GAPDH was used as internal control. Representative data are from 3 independent experiments. *, $P < 0.01$. F, immunohistochemistry of versican on CD11b$^+$Ly6G^{high} and CD11b$^+$Ly6C^{high} cells. Hematoxylin (Hem) was used to determine the morphology of the nucleus. G, Western blot analysis showing versican in sorted CD11b$^+$Ly6G^{high} and CD11b$^+$Ly6C^{high} cells from metastatic lungs of MMTV-PyMT mice.

including subsets of T and B cells (Fig. 2B). Consistent with RT-PCR, Western blot analysis showed elevated versican protein in the metastatic lung compared with wild-type controls (Fig. 2C).

Flow cytometric analysis showed that the CD11b$^+$Gr1$^+$ cells are composed of CD11b$^+$Ly6C^{high} and CD11b$^+$Ly6G^{high} subpopulations (Fig. 2D; refs. 20–22) and their recruitment increased as a function of metastatic progression (Supplementary Fig. S2A and S2B). Interestingly, versican expression was confined to the Ly6C^{high} cells (Fig. 2E). Nuclear morphology analysis showed that the CD11b$^+$Ly6C^{high} cells are mononuclear, whereas the CD11b$^+$Ly6G^{high} cells are polymorphonuclear (Fig. 2F). Consistently, versican protein was also detected in the mononuclear CD11b$^+$Ly6C^{high} cells by immunohistochemical (IHC) and Western blot analyses (Fig. 2F and G). In the primary tumors, versican was also confined to the low abundance CD11b$^+$Ly6C^{high} myeloid cells, whereas the abundant CD11b$^+$F4/80$^+$ myeloid cells did not express versican (Supplementary Fig. S3).

Contrary to previous studies using cultured cell lines (23–25), endothelial cells and the fibroblasts did not show significant versican levels compared with CD11b$^+$Ly6C^{high} cells in the metastatic lungs (Supplementary Fig. S4A). Importantly, the contribution of fibroblasts to the metastatic lung was about 10-fold lower compared with CD11b$^+$Ly6C^{high} cells, and no significant increase in numbers was observed in the metastatic lungs compared with controls (Supplementary Fig. S4B).

Published OnlineFirst January 26, 2012; DOI: 10.1158/0008-5472.CAN-11-2905

Furthermore, analysis a panel of tumor cell lines showed significantly lower versican expression compared with sorted myeloid cells (Supplementary Fig. S4C). Taken together, these results suggest that the Ly6C^{high} myeloid cells are the major contributors of versican in metastatic lungs.

Versican suppression in myeloid cells impairs lung metastases

To explore the role of myeloid cell–derived versican in pulmonary metastasis, we conducted versican knockdown in bone marrow cells *in vivo*. Given that versican is confined to the CD11b^{+}Ly6C^{high} myeloid cells, we reasoned that versican knockdown in total bone marrow cells would only impact the Ly6C^{high} cells, thereby providing exquisite specificity. Two shRNAs specifically targeting exon 8 (V0/V1-specific exon) were generated (Supplementary Fig. S5A and S5B), which effectively reduced endogenous versican (V0/V1) expression as compared with nonspecific shRNA control (Supplementary Fig. S5C).

Versican-specific shRNA (shVcn) or nonspecific shRNA (shNS) was introduced via lentiviruses into lineage wild-type–negative (Lin^{-}) bone marrow progenitor cells and then transplanted into lethally irradiated MMTV-PyMT recipient mice (4 weeks old) as described in our previous studies (8, 12). Successful bone marrow reconstitution was confirmed by flow cytometric analysis of transplanted recipient mice (Supplementary Fig. S6A). In the lungs, as expected, versican expression was upregulated (>3-fold) in shNS-BMT MMTV-PyMT mice compared with controls (Supplementary Fig. S6B). However, versican expression was inhibited in shVcn-BMT mice (Supplementary Fig. S6B). Versican knockdown in the recruited Gr1^{+} cells in the lungs of shVcn-BMT mice (Fig. 3A and B),

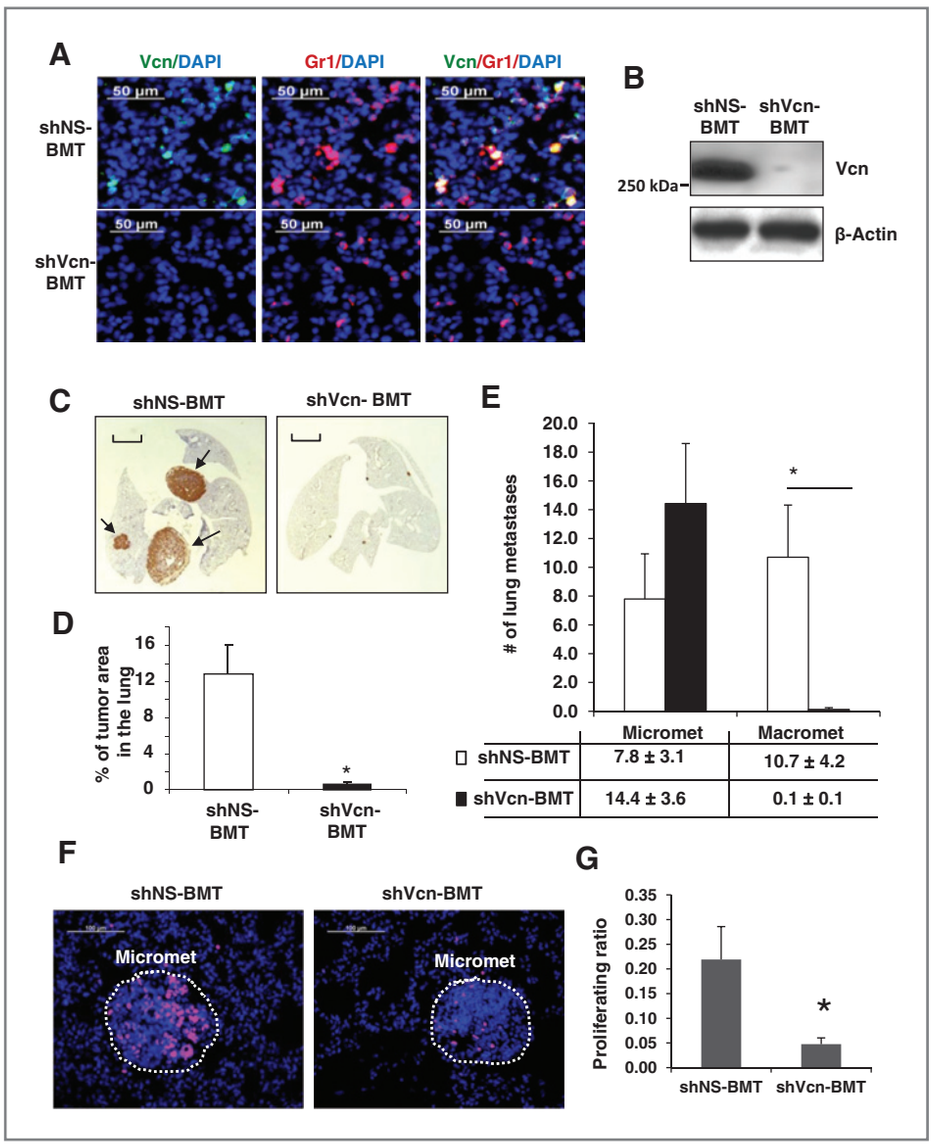

Figure 3. Versican (Vcn) deficiency in myeloid cells impairs macrometastases in MMTV-PyMT mice. A, representative microscopy images showing versican (green) deficiency in Gr1^{+} (red) cells in the lungs of shVcn-BMT MMTV-PyMT mice compared with shNS-BMT mice (10 weeks old). DAPI, 4′,6-diamidino-2-phenylindole. B, Western blot analyses showing versican in the lungs from shNS-BMT and shVcn-BMT MMTV-PyMT mice. C, representative lung images (stained with anti-PyMT antibody) of shNS-BMT and shVcn-BMT MMTV-PyMT mice (15 weeks old). Arrows mark pulmonary metastases. Scale bar, 2 mm. D, quantitation of the area of metastases in shNS-BMT and shVcn-BMT MMTV-PyMT mice (15 weeks old, $n = 7$–9 per group; *, $P < 0.01$ as compared with shNS-BMT group). E, quantitation of the number of metastases in shNS-BMT and shVcn-BMT MMTV-PyMT mice. The average number of micrometastasis (<1 mm in diameter) and macrometastasis (>1 mm in diameter) were counted from at least 5 sections from individual animals, $n = 7$–9; *, $P < 0.01$ as compared with shNS-BMT group. F, staining of Ki67 (magenta) showing proliferating cells in the micrometastases in lungs of shNS-BMT mice as compared with that from shVcn-BMT mice. G, quantification of the proliferation ratio in micrometastases showing less proliferating cells in lesions from shVcn-BMT mice compared with shNS-BMT mice. $n = 10$; *, $P < 0.01$.

Published OnlineFirst January 26, 2012; DOI: 10.1158/0008-5472.CAN-11-2905

resulted in impaired lung metastases compared with shNS-BMT controls (0.60% ± 0.25% vs. 12.8% ± 3.2%, respectively; Fig. 3C and D). IHC examination of the lungs from shVcn-BMT animals showed severe impairment of macrometastases while micrometastases remained unaffected (Fig. 3E, Supplementary Fig. S7), whereas the primary breast tumors remained unaffected in these mice. Taken together, these results show that versican deficiency in the recruited myeloid cells significantly impaired tumor outgrowth at the metastatic site.

Myeloid cell–derived versican enhances proliferation of metastatic tumor cells to promote outgrowth

Versican knockdown did not affect the recruitment of $CD11b^+Gr1^+$ myeloid cells in the lung microenvironment as determined by immunostaining (Fig. 3A) and flow cytometry (15.8% ± 1.9% in shRNA-BMT vs. 15.3% ± 4.2% in shVcn-BMT mice; Supplementary Fig. S8A and S8B), nor did it perturb the recruitment of other bone marrow cells including B cells ($B220^+$) or T cells ($CD3^+$; Supplementary Fig. S8A and S8B). As expected, the immune microenvironment of the lungs remained unperturbed as a result of versican knockdown as evaluated by expression of key mediators including TNF-α, interleukin (IL)-1, IL-6, IL-4, IL-10, arginase 1, arginase 2, and NOS2 (Supplementary Fig. S8C), suggesting that versican deficiency did not affect myeloid-derived suppressor cell (MDSC) activity of myeloid cells. Taken together, these results suggest a novel function for these myeloid progenitor cells in promoting metastases.

Previous studies have shown that versican V1 promotes cell proliferation in NIH3T3 fibroblasts (25). Therefore, we posited that versican expressed by recruited myeloid cells might enhance proliferation of metastatic tumor cells to promote tumor outgrowth. Consistent with this hypothesis, abundant $Ki67^+$ proliferating cells were observed in metastatic lesions in shNS-BMT mice where versican was available, compared with metastatic lesions from shVcn-BMT mice where versican expression was suppressed (Fig. 3F and G; Supplementary Fig. S9A).

Taken together, these results show that versican deficiency in the bone marrow does not affect the recruitment of $CD11b^+Gr1^+$ cells and other immune cells to the lung microenvironment. However, versican expressed by these myeloid cells promotes metastatic tumor outgrowth by enhancing cell proliferation.

Versican promotes proliferation and induces MET of metastatic tumor cells

To further evaluate the cell proliferation promoting function of versican, we used metastatic human breast cancer cells, MDA-MB-231. To mirror the paracrine effects of versican secreted by myeloid cells on metastatic tumor cells *in vitro*, we generated conditioned media from flow cytometry–sorted $CD11b^+Gr1^+$ cells from the lungs of tumor-bearing mice. Administration of the Gr1 conditioned media to MDA-MB-231 cells increased cells in S-phase compared with controls (Fig. 4A). Consistently, the proliferation rate of MDA-MB-231 cells was enhanced following expression of a secreted form (10) of versican V1 isoform (12.1% and 5.4% of S-phase cells with and without versican, respectively; Supplementary Fig. S9B).

Interestingly, versican-induced proliferation increase in MDA-MB-231 cells treated with Gr1 conditioned media was associated with the acquisition of an epithelial phenotype as indicated by upregulation of epithelial cell markers including E-cadherin and occludin and a concomitant inhibition of the mesenchymal marker vimentin (Fig. 4B). These results suggested that an MET had occurred in these cells, presumably mediated by versican present in the Gr1 conditioned media. To confirm this, we treated MDA-MB-231 cells with biochemically purified versican (V1 isoform; Supplementary Fig. S10A and S10B), and observed induction of MET (Fig. 4B). In agreement with this observation, MDA-MB-231 cell expressing a secreted form of versican (V1 isoform) established aggregated cobblestone-like colonies (Fig. 4C, phase-contrast; top and bottom) and showed induction of epithelial and suppression of mesenchymal markers as determined by immunostaining, Western blot, and RT-PCR analysis (Fig. 4C and D; Supplementary Fig. S11). Importantly, versican attenuated phospho (p)-Smad2 levels in MDA-MB-231 cells, whereas the levels of total Smad2/3 remained unchanged (Fig. 4D). Given that p-Smad2 is a regulator of key EMT-promoting transcription factors including Snail, it is plausible that versican-mediated attenuation of p-Smad2 levels (Fig. 4D) and suppression of Snail (Supplementary Fig. S11) in MDA-MB-231 cells may have inhibited the TGF-β/Smad2/3 signaling pathway, a well-known stimulator of EMT in various tumors (26–29). These results suggest that versican-mediated blockade of the TGF-β/Smad2 pathway may stimulate MET, resulting in increased cell proliferation which collectively promotes focal tumor outgrowth at the metastatic site.

Versican deficiency inhibits metastases *in vivo* by blocking MET

In tumor progression, EMT confers an invasive and metastatic phenotype that supports escape of tumor cells from the primary tumor site. It is speculated that subsequently, the disseminated mesenchymal tumor cells must undergo the reverse transition, MET, at the site of metastasis, as metastases recapitulate the pathology of their corresponding primary tumors (9, 30, 31). However, MET has not been accurately recapitulated in breast cancer metastasis. To assess if MET occurs *in vivo*, we inoculated MDA-MB-231 cells that exhibit a typical mesenchymal phenotype ($E\text{-cadherin}^-/\text{vimentin}^+$) in severe combined immunodeficient (SCID) mice and allowed metastases to develop in the lungs. Notably, MDA-derived metastases exhibited an $E\text{-cadherin}^+$ epithelial phenotype (Supplementary Fig. S12A and S12B), suggesting that MDA-MB-231 cells have undergone MET in the lung environment. In this context, analysis of lung metastases from patients with breast cancer also showed $E\text{-cadherin}^+$ and vimentin^- metastases (Supplementary Fig. S12C). On the basis of these observations, we hypothesized that myeloid cells recruited in the premetastatic lungs produce versican which induces MET in tumor cells to promote tumor outgrowth.

To determine whether versican-mediated MET is necessary for metastases formation *in vivo*, we injected luciferase-RFP–

Published OnlineFirst January 26, 2012; DOI: 10.1158/0008-5472.CAN-11-2905

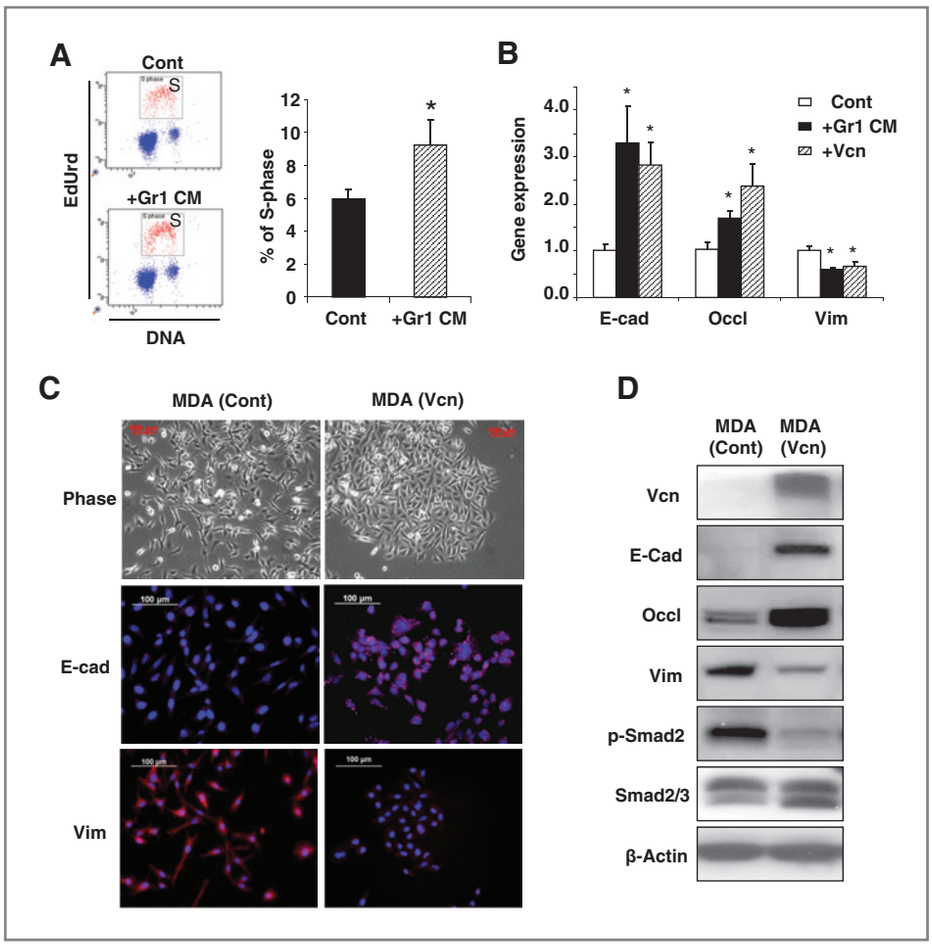

Figure 4. Versican enhances proliferation and induces MET in metastatic tumor cells. A, flow cytometric plots depicting cell-cycle analysis of metastatic breast cancer MDA-MB-231 cells treated with $Gr1^+$ conditioned media (CM) or control media (Cont). Percentage of S-phase cells is indicated. Representative plots are from 3 experiments. B, quantitative RT-PCR analysis of epithelial/mesenchymal marker expression in MDA-MB-231 cells treated with Gr1 CM or biochemically purified versican (+Vcn, 2.5 μg/mL). $n = 3$; *, $P < 0.01$ as compared with untreated cells (Cont). Occl, occludin. C, microscopic images of MDA-control cells and MDA-versican cells (MDA-Vcn) depicting morphology (phase) and expression of epithelial/mesenchymal markers. E-cad, E-cadherin; Vim, vimentin. D, Western blot analysis of versican (>250 kDa), EMT markers, phospho (p)-Smad2, and total Smad2/3 expression in MDA (Vcn) cells and MDA (Cont) cells. Representative data from 3 experiments.

labeled MDA-MB-231 cells via tail vein in SCID mice and monitored metastases progression either in the presence of versican (control IgG–treated mice) or in lack of versican-producing myeloid cells (anti-Gr1–treated mice). Depletion of $Gr1^+$ myeloid cells significantly impaired progression of metastases by more than 5-fold (Fig. 5A and B). Of note, the anti-Gr1 antibody treatment significantly inhibited the upregulated versican expression in the metastatic lungs (Fig. 5C). Further evaluation of the lungs showed that macroscopic E-$cadherin^+$/$vimentin^{low}$ metastatic lesions were generated by MDA-MB-231 cells in the presence of versican (Fig. 5D, top) as expected. However, versican deficiency resulted in microscopic $vimentin^{high}$/E-$cadherin^-$ lesions (Fig. 5D, bottom) indicating a failure of MET. To confirm that the MET-induced accelerated metastasis was mainly due to versican, we carried out a versican gain-of-function experiment. We injected MDA-MB-231 cell expressing a secreted form of versican V1 isoform (MDA-Vcn) and MDA-Cont cells via tail vein in SCID mice. Bioluminescence imaging analysis revealed accelerated progression (>4-fold) of lung metastases with MDA-Vcn cells compared with MDA-Cont cells (Fig. 5E and F).

Taken together, these results suggest that versican promotes MET of metastatic tumor cells and enhances progression into macrometastatic lesions.

Myeloid cells express versican in the metastatic lungs of breast cancer patients

Next, we asked whether metastatic lungs of patients with breast cancer exhibit elevated levels of versican as observed in mouse models. IHC analysis showed enhanced versican in the metastatic lungs of patients with breast cancer but not in lungs of normal healthy controls (Fig. 6A). IHC analysis of metastatic lungs showed that versican expression was confined to the vicinity of $CD11b^+$ myeloid cell clusters (Fig. 6B). Using a cohort of patients with breast cancer who have developed lung ($n = 6$) or liver ($n = 11$) metastases, we quantified versican expression by RT-PCR. Significantly higher versican expression was detected in metastatic organs than in normal tissues (5.8 ± 1.3- and 6.5 ± 1.5-fold in the liver and lung metastasis, respectively; Fig. 6C). We further evaluated whether a subset of $CD11b^+$ cells expressed versican in patients with cancer. Given that Gr1 is not expressed in humans, myeloid cells are defined by the coexpression of CD11b and CD33 (20). Indeed, flow cytometric analysis showed that the $CD11b^+CD33^+$ cells that comprise the monocytic population expressed versican, whereas the $CD11b^+CD33^-$ fraction or the pure tumor cells did not (Fig. 6D and E). These results suggest that as observed in mouse models, versican expressed by tumor-elicited myeloid cells may contribute to metastasis in patients with cancer.

Published OnlineFirst January 26, 2012; DOI: 10.1158/0008-5472.CAN-11-2905

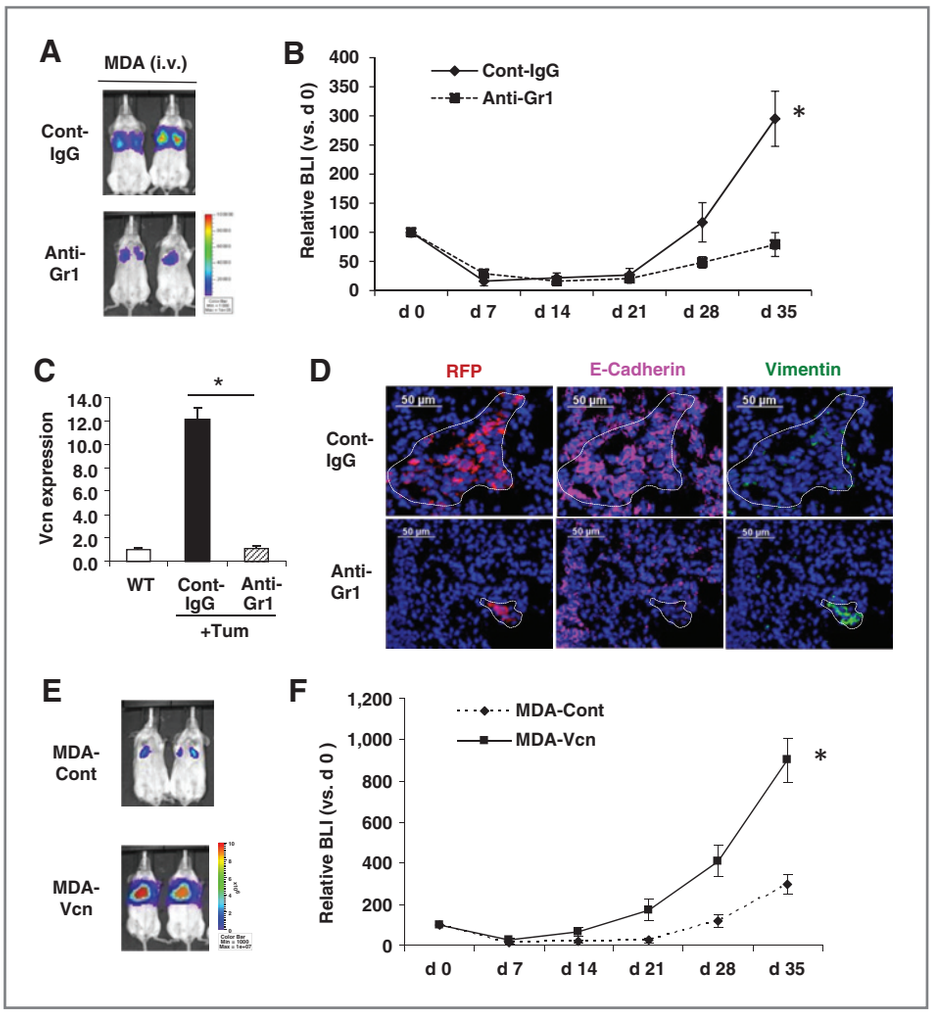

Figure 5. Versican deficiency impairs MET-mediated lung metastases *in vivo*. A, bioluminescent images (BLI) showing that depletion of versican-producing $Gr1^+$ cells by anti-Gr1 antibody treatment inhibited lung metastases formed by MDA-MB-231 cells compared with IgG-treated controls. Scale bar depicts the photon flux (photons/s). B, quantification of pulmonary metastases by BLI at days 0, 7, 14, 21, 28, and 35 after inoculation. The relative BLIs are normalized using the values from day 0. $n = 10$; *, $P < 0.01$. C, myeloid cells harvested from wild-type (WT) and control antibody–treated (Cont-IgG) or anti-Gr1 antibody–treated (Anti-Gr1) tumor-bearing animals (+Tum). Versican expression was analyzed by RT-PCR ($n = 3$ in each group). GAPDH (glyceraldehyde-3-phosphate dehydrogenase) was used as internal control for RT-PCR. *, $P < 0.01$ as indicated. D, images showing expression of E-cadherin (magenta) and vimentin (green) in pulmonary metastases formed by MDA-MB-231 cells in mice treated with control IgG or anti-Gr1 antibodies. Tumor cells were detected by the intrinsic RFP signal (red). The metastatic lesions are shown within the dotted line. Note that lung epithelial cells surrounding the metastases also stain for E-cadherin. E, versican promotes lung metastasis *in vivo*. Representative BLIs showing accelerated metastases of MDA-Vcn cells in the lung after tail vein injection as compared with MDA-Cont cells ($n = 5$). F, quantification of pulmonary metastases by BLI at days 0, 7, 14, 21, 28, and 35 after inoculation. The relative BLIs are normalized using the values from day 0. $n = 5$; *, $P < 0.01$.

Discussion

We have shown that bone marrow–derived $CD11b^+GR1^+$ myeloid progenitor cells recruited to the premetastatic lungs promote tumor outgrowth. Various protumorigenic activities have been associated with $Gr1^+$ myeloid cells, including expression of proangiogenic factor BV8 (32), metastasis-promoting lysyl oxidase and matrix metalloproteinase 9 (MMP9; ref. 33), contribution to TGF-β–mediated metastasis (34), and immune tolerance and suppression by virtue of innate MDSC activity (35, 36). Here, we have identified a novel role for the recruited $Gr1^+$ myeloid cells in mediating tumor outgrowth in metastatic lungs. By secreting versican, the $Ly6C^{high}$ monocytic subpopulation of $Gr1^+$ myeloid cells, in a paracrine fashion, promoted cell proliferation and induced MET of tumor cells (Fig. 7). Importantly, versican deficiency in the $Gr1^+$ cells did not block their recruitment to the lung microenvironment; neither did it alter the immune microenvironment of the lung as determined by evaluation of key cell types and immune mediators suggesting that the MDSC activity of these cells was not compromised. However, versican knockdown in myeloid cells or specific depletion of versican-producing myeloid cells significantly impaired macrometastases formation.

In the metastatic lungs, the major contributors of versican were $CD11b^+Ly6C^{high}$ cells. While the fibroblasts expressed

Published OnlineFirst January 26, 2012; DOI: 10.1158/0008-5472.CAN-11-2905

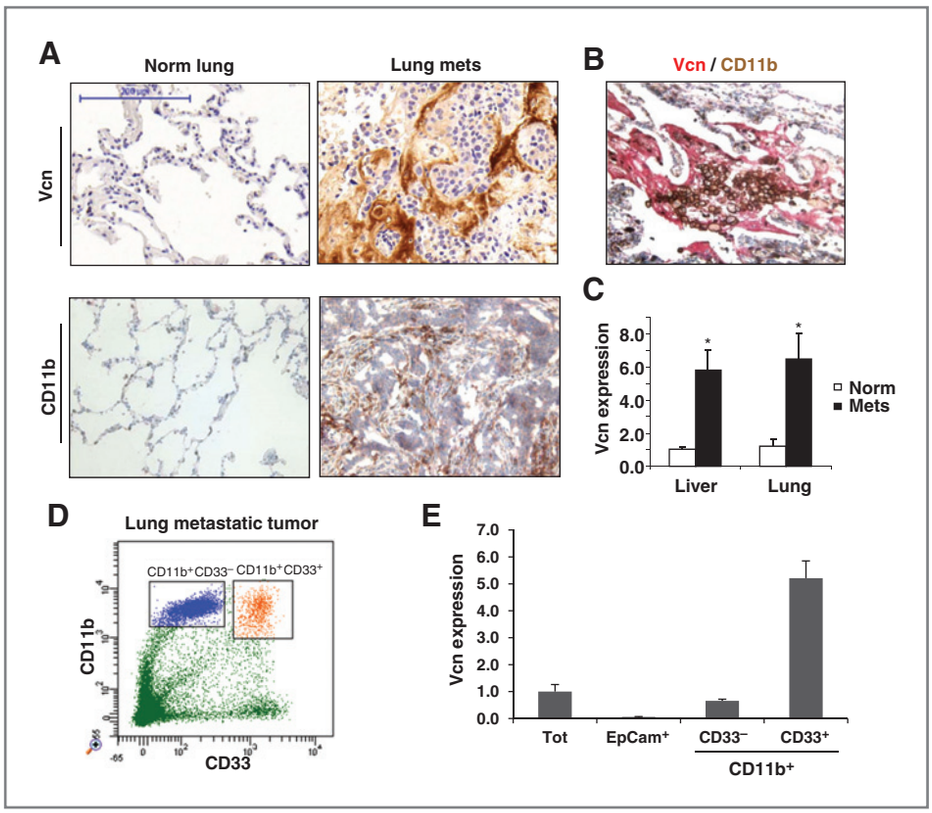

Figure 6. Versican expression in the metastatic tumors of patients with breast cancer. A, representative IHC images of lungs from normal healthy subjects (Normal Lung, $n = 5$) and patients with breast cancer with metastases (Lung Mets, $n = 11$) showing stromal versican expression. Scale bar, 200 μm. B, immunohistochemistry of lung metastases from a patient with breast cancer showing colocalization of recruited $CD11b^+$ (brown) myeloid cells with versican (red). C, quantification of versican expression by RT-PCR in lung metastases ($n = 6$) and liver metastases ($n = 11$) of patients with breast cancer as compared with healthy normal (norm) tissues ($n = 5$ and $n = 4$, respectively). *, $P < 0.01$. D, flow cytometry showing that $CD11b^+$ cells in the human metastatic lungs are composed of $CD11b^+CD33^+$ and $CD11b^+CD33^-$ populations. E, RT-PCR of versican expression in sorted total cells (Tot), tumor cells ($EpCam^+$), $CD11b^+CD33^+$ myeloid cells, and $CD11b^+CD33^-$ cells in a patient with breast cancer with lung metastases.

versican as observed in previous studies (23–25), the contribution of fibroblasts to the metastatic lung was about 10-fold lower compared with $CD11b^+Ly6C^{high}$ cells, and no significant increase in numbers was observed in the metastatic lungs compared with controls (Supplementary Fig. S4B). Consistent with these observations, versican knockdown specifically in the bone marrow significantly impaired lung metastasis *in vivo*. However, in one report, versican expression by Lewis lung carcinoma (LLC) cells promoted metastasis (37). Our analysis of a panel of tumor cell lines from breast, prostate, colon, and lung cancer showed that versican expression in tumor cells is significantly lower compared with myeloid cells. On the basis of all these results, we conclude that the $Ly6C^{high}$ myeloid cells are the major contributors of versican in metastatic lungs in both mouse and human (Figs. 2 and Fig. 6 and Supplementary Fig. S4C). MET plays an important role in development (38);

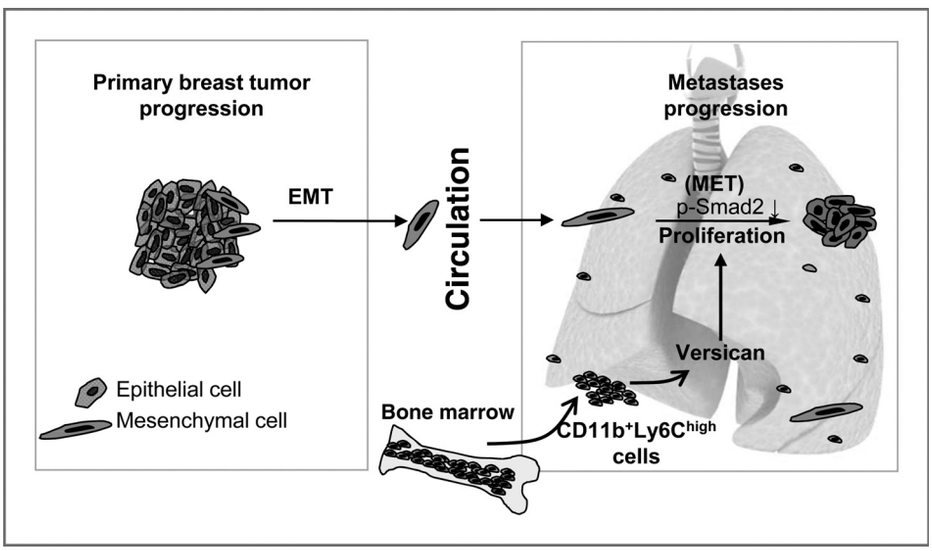

Figure 7. Schematic depicting the contribution of bone marrow–derived myeloid cells to the formation of lung metastases from breast tumor. BM, bone marrow.

Published OnlineFirst January 26, 2012; DOI: 10.1158/0008-5472.CAN-11-2905

however, the MET cascade has not been shown in tumor metastasis. In this study, we have observed E-cadherin$^+$ and vimentin$^-$ metastatic lesions in both mice and human. Consistently, in a recent study, IHC analysis of many human primary lung tumors and their brain metastases showed increased epithelial to mesenchymal ratios in metastatic lesions compared with advanced primary tumors (39). Thus, our observation that versican stimulates MET of metastatic tumor cells explains, in part, the observations that cancer cells in distant metastases exhibit an epithelial phenotype resembling the primary tumor from which they arose. Our study has also addressed the speculation in the field that metastatic tumor cells recruited to distal target organs undergo a reverse EMT often referred to as MET (9, 30, 31). However, technological limitations, such as lack of robust markers, to track single disseminated tumor cells that have undergone EMT to the metastatic site in patients preclude a detailed analysis of MET in humans, further exacerbated with limitations in noninvasive dynamic imaging at the single-cell level.

We have also explored the mechanism by which versican induces MET. Versican attenuated the Smad-mediated EMT signaling pathway as determined by the reduction of p-Smad2 levels and suppression of transcription factor Snail. The suppression of Smad2 pathway–induced MET increased cell proliferation consistent with previous reports (40, 41). In addition, versican did not impact apoptosis (data not shown), suggesting that versican-mediated stimulation of MET and enhanced proliferation may be the main mechanisms of increased tumor outgrowth and formation of focal macrometastases. Analysis of a cohort of patients with breast cancer from whom distal metastases were available showed clusters of myeloid cells expressing versican in the metastatic lungs. Consistent with immunohistochemistry, RT-PCR analysis showing enhanced versican expression in metastatic lungs, brain, and liver in patients with breast cancer compared with control normal lungs. These observations suggest that versican expression in the metastatic organ may be used to predict survival, given the relationship between metastases and poor survival in patients with breast cancer. However, such an analysis is challenging at the present time due to limited availability of human metastatic lesions, and future studies are required to expand the analysis in a much larger cohort of patients with breast cancer to determine with statistical confidence whether increased levels of versican expression in the lungs correlate with poor survival.

Given that the initial colonization by disseminated tumor cells has occurred in many patients at the time of primary tumor diagnosis, our results suggest that selectively targeting tumor-elicited myeloid cells or versican-mediated proliferation pathways, perhaps in combination with conventional chemotherapeutics, may represent a potential therapeutic strategy for combating metastatic disease.

Disclosure of Potential Conflicts of Interest

No potential conflicts of interests were disclosed by other authors.

Acknowledgments

The authors thank Drs. Zimmermann (University of Zurich) for human versican cDNA clone and Anna Durrans for valuable comments on the manuscript.

Grant Support

The work was partly supported by Neuberger Berman Lung Cancer Laboratory, the Robert I. Goldman Foundation, and Cornell Center on the Microenvironment and Metastasis through Award Number U54CA143876 from the National Cancer Institute (V. Mittal).

The costs of publication of this article were defrayed in part by the payment of page charges. This article must therefore be hereby marked *advertisement* in accordance with 18 U.S.C. Section 1734 solely to indicate this fact.

Received August 29, 2011; revised December 20, 2011; accepted January 11, 2012; published OnlineFirst January 26, 2012.

References

1. Townson JL, Chambers AF. Dormancy of solitary metastatic cells. Cell Cycle 2006;5:1744–50.
2. Naumov GN, Bender E, Zurakowski D, Kang SY, Sampson D, Flynn E, et al. A model of human tumor dormancy: an angiogenic switch from the nonangiogenic phenotype. J Natl Cancer Inst 2006;98:316–25.
3. Gupta GP, Massague J. Cancer metastasis: building a framework. Cell 2006;127:679–95.
4. Joyce JA, Pollard JW. Microenvironmental regulation of metastasis. Nat Rev Cancer 2009;9:239–52.
5. Polyak K, Weinberg RA. Transitions between epithelial and mesenchymal states: acquisition of malignant and stem cell traits. Nat Rev Cancer 2009;9:265–73.
6. Fidler IJ. The pathogenesis of cancer metastasis: the `seed and soil' hypothesis revisited. Nat Rev Cancer 2003;3:453–8.
7. Kaplan RN, Psaila B, Lyden D. Bone marrow cells in the `pre-metastatic niche': within bone and beyond. Cancer Metastasis Rev 2006;25:521–9.
8. Gao D, Nolan DJ, Mellick AS, Bambino K, McDonnell K, Mittal V. Endothelial progenitor cells control the angiogenic switch in mouse lung metastasis. Science 2008;319:195–8.
9. Chaffer CL, Thompson EW, Williams ED. Mesenchymal to epithelial transition in development and disease. Cells Tissues Organs 2007;185:7–19.
10. Dutt S, Cassoly E, Dours-Zimmermann MT, Matasci M, Stoeckli ET, Zimmermann DR. Versican V0 and V1 direct the growth of peripheral axons in the developing chick hindlimb. J Neurosci 2011;31:5262–70.
11. Guy CT, Cardiff RD, Muller WJ. Induction of mammary tumors by expression of polyomavirus middle T oncogene: a transgenic mouse model for metastatic disease. Mol Cell Biol 1992;12:954–61.
12. Nolan DJ, Ciarrocchi A, Mellick AS, Jaggi JS, Bambino K, Gupta S, et al. Bone marrow-derived endothelial progenitor cells are a major determinant of nascent tumor neovascularization. Genes Dev 2007;21:1546–58.
13. Wight TN. Versican: a versatile extracellular matrix proteoglycan in cell biology. Curr Opin Cell Biol 2002;14:617–23.
14. Ricciardelli C, Brooks JH, Suwiwat S, Sakko AJ, Mayne K, Raymond WA, et al. Regulation of stromal versican expression by breast cancer cells and importance to relapse-free survival in patients with node-negative primary breast cancer. Clin Cancer Res 2002;8:1054–60.
15. Suwiwat S, Ricciardelli C, Tammi R, Tammi M, Auvinen P, Kosma VM, et al. Expression of extracellular matrix components versican, chondroitin sulfate, tenascin, and hyaluronan, and their association with disease outcome in node-negative breast cancer. Clin Cancer Res 2004;10:2491–8.
16. Pukkila M, Kosunen A, Ropponen K, Virtaniemi J, Kellokoski J, Kumpulainen E, et al. High stromal versican expression predicts

Published OnlineFirst January 26, 2012; DOI: 10.1158/0008-5472.CAN-11-2905

unfavourable outcome in oral squamous cell carcinoma. J Clin Pathol 2007;60:267–72.
17. Kodama J, Hasengaowa, Kusumoto T, Seki N, Matsuo T, Ojima Y, et al. Prognostic significance of stromal versican expression in human endometrial cancer. Ann Oncol 2007;18:269–74.
18. Pirinen R, Leinonen T, Bohm J, Johansson R, Ropponen K, Kumpulainen E, et al. Versican in nonsmall cell lung cancer: relation to hyaluronan, clinicopathologic factors, and prognosis. Hum Pathol 2005;36:44–50.
19. Pukkila MJ, Kosunen AS, Virtaniemi JA, Kumpulainen EJ, Johansson RT, Kellokoski JK, et al. Versican expression in pharyngeal squamous cell carcinoma: an immunohistochemical study. J Clin Pathol 2004;57:735–9.
20. Krystal G, Sly L, Antignano F, Ho V, Ruschmann J, Hamilton M. Re: The terminology issue for myeloid-derived suppressor cells. Cancer Res 2007;67:3986.
21. Gabrilovich DI, Bronte V, Chen SH, Colombo MP, Ochoa A, Ostrand-Rosenberg S, et al. The terminology issue for myeloid-derived suppressor cells. Cancer Res 2007;67:425; author reply 426.
22. Coffelt SB, Lewis CE, Naldini L, Brown JM, Ferrara N, De Palma M. Elusive identities and overlapping phenotypes of proangiogenic myeloid cells in tumors. Am J Pathol 2010;176:1564–76.
23. Ricciardelli C, Sakko AJ, Ween MP, Russell DL, Horsfall DJ. The biological role and regulation of versican levels in cancer. Cancer Metastasis Rev 2009;28:233–45.
24. Zimmermann DR, Ruoslahti E. Multiple domains of the large fibroblast proteoglycan, versican. EMBO J 1989;8:2975–81.
25. Sheng W, Wang G, Wang Y, Liang J, Wen J, Zheng PS, et al. The roles of versican V1 and V2 isoforms in cell proliferation and apoptosis. Mol Biol Cell 2005;16:1330–40.
26. Padua D, Massague J. Roles of TGFbeta in metastasis. Cell Res 2009;19:89–102.
27. Shi Y, Massague J. Mechanisms of TGF-beta signaling from cell membrane to the nucleus. Cell 2003;113:685–700.
28. Song J. EMT or apoptosis: a decision for TGF-beta. Cell Res 2007;17:289–90.
29. Hata A, Shi Y, Massague J. TGF-beta signaling and cancer: structural and functional consequences of mutations in Smads. Mol Med Today 1998;4:257–62.
30. Hugo H, Ackland ML, Blick T, Lawrence MG, Clements JA, Williams ED, et al. Epithelial–mesenchymal and mesenchymal–epithelial transitions in carcinoma progression. J Cell Physiol 2007;213:374–83.
31. Chaffer CL, Brennan JP, Slavin JL, Blick T, Thompson EW, Williams ED. Mesenchymal-to-epithelial transition facilitates bladder cancer metastasis: role of fibroblast growth factor receptor-2. Cancer Res 2006;66:11271–8.
32. Kowanetz M, Wu X, Lee J, Tan M, Hagenbeek T, Qu X, et al. Granulocyte-colony stimulating factor promotes lung metastasis through mobilization of Ly6G+Ly6C +granulocytes. Proc Natl Acad Sci U S A 2010;107:21248–55.
33. Erler JT, Bennewith KL, Cox TR, Lang G, Bird D, Koong A, et al. Hypoxia-induced lysyl oxidase is a critical mediator of bone marrow cell recruitment to form the premetastatic niche. Cancer Cell 2009;15:35–44.
34. Yang L, Huang J, Ren X, Gorska AE, Chytil A, Aakre M, et al. Abrogation of TGF beta signaling in mammary carcinomas recruits Gr-1+CD11b +myeloid cells that promote metastasis. Cancer Cell 2008;13:23–35.
35. Ostrand-Rosenberg S, Sinha P. Myeloid-derived suppressor cells: linking inflammation and cancer. J Immunol 2009;182:4499–506.
36. Youn JI, Nagaraj S, Collazo M, Gabrilovich DI. Subsets of myeloid-derived suppressor cells in tumor-bearing mice. J Immunol 2008;181:5791–802.
37. Kim S, Takahashi H, Lin WW, Descargues P, Grivennikov S, Kim Y, et al. Carcinoma-produced factors activate myeloid cells through TLR2 to stimulate metastasis. Nature 2009;457:102–6.
38. Vainio S, Lin Y. Coordinating early kidney development: lessons from gene targeting. Nat Rev Genet 2002;3:533–43.
39. Prudkin L, Liu DD, Ozburn NC, Sun M, Behrens C, Tang X, et al. Epithelial-to-mesenchymal transition in the development and progression of adenocarcinoma and squamous cell carcinoma of the lung. Mod Pathol 2009;22:668–78.
40. Mur C, Martínez-Carpio PA, Fernández-Montolí ME, Ramon JM, Rosel P, Navarro MA. Growth of MDA-MB-231 cell line: different effects of TGF-beta(1), EGF and estradiol depending on the length of exposure. Cell Biol Int 1998;22:679–84.
41. Zugmaier G, Ennis BW, Deschauer B, Katz D, Knabbe C, Wilding G, et al. Transforming growth factors type beta 1 and beta 2 are equipotent growth inhibitors of human breast cancer cell lines. J Cell Physiol 1989;141:353–61.

Published OnlineFirst January 26, 2012; DOI: 10.1158/0008-5472.CAN-11-2905

Cancer Research
The Journal of Cancer Research (1916–1930) | The American Journal of Cancer (1931–1940)

AACR American Association for Cancer Research

Myeloid Progenitor Cells in the Premetastatic Lung Promote Metastases by Inducing Mesenchymal to Epithelial Transition

Dingcheng Gao, Natasha Joshi, Hyejin Choi, et al.

Cancer Res 2012;72:1384-1394. Published OnlineFirst January 26, 2012.